Anadolu Üniversitesi Bilim ve Teknoloji Dergisi A- Uygulamalı Bilimler ve Mühendislik
Anadolu University Journal of Science and Technology A- Applied Sciences and Engineering

2017 - Volume: 18 Number: 4
Page: 788-803
DOI: 10.18038/aubtda.340842
Received: 03 March 2017 Revised: 04 August 2017 Accepted: 15 August 2017

PRECISE CONTROL OF AN ELECTROMECHANICALLY-ACTUATED LAUNCHER UNDER PARAMETER UNCERTAINTY

Hamza KAMİŞLİ [1], Metin U. SALAMCI [2], Bülent ÖZKAN [1,*]

[1] The Scientific and Technological Research Council of Turkey, Defense Industry Research and Development Institute (TÜBİTAK SAGE), Ankara, Turkey
[2] Mechanical Engineering Department, Gazi University, Ankara, Turkey

ABSTRACT

Dynamic modeling and control of two-degree-of-freedom launchers which are utilized for launching munitions such as missiles and rockets have become one of the most popular fields in recent years. Control of launch vehicles gains more importance especially when they are mounted on moving vehicles. In this study, the mathematical modeling and control with parameter uncertainties of a high-accuracy two-degree-of-freedom electromechanically-actuated launcher are investigated in the direction of reducing the impact impulse on the control system. In this context, after the dynamic equations of the system are derived, the design of convenient control systems is carried out so as to reduce the undesired contribution of the thrust effect. In control, computed torque and proportional, integral, and derivative (PID) and computed torque and sliding mode control algorithms, and computed torque and sliding mode control cascaded control algorithms are developed by taking the parameter uncertainties into consideration. In the conclusion part, the performance characteristics of these controllers are compared and it is shown that the cascaded control scheme yields more satisfactory results in accurate position control. In the computer simulations conducted in this extent, the MATLAB® software and its SIMULINK® module are utilized.

Keywords: Electromechanically-actuated launcher, Launcher control, Computed torque, Sliding mode, Parameter uncertainty.

1. INTRODUCTION

In order to protect the military land vehicles against external threats including both guided and unguided munition, one of the approaches is to mount launchers upon them. This way, it is aimed to defeat them or at least to minimize their collateral damage on the land vehicles. The systems operating based on the mentioned method are called the active protection systems (APSs). Depending on how they are implemented, APSs can be categorized into two main groups: ‘soft kill' and 'hard kill' systems. In the soft kill applications, the threat is prevented from harming the platform under consideration by means of soft tools such as radar signals and it is not physically destructed. Conversely, the destruction of the threat by means of projectiles, rockets, or missiles which are fired from the launchers constitutes the main objective in the hard kill approach. Regarding its effectiveness along with the experience gained in the past, the hard kill-type APS is the preferred one. In this method, it is desired that the enemy munition involving missiles or rockets be destructed at a distance very close to the platform to be protected right after it is detected by means of radar antennas and recognizing using convenient means. Namely, the intended demolition distance of the threat varies between 10 and 150 meters. In order for the APS to be successful under this circumstance, it should react the external threat within a time span shorter than 1 second [1,2].

Looking at the relevant literature, it is observed that there are few studies conducted on the control of the launchers while several works are encountered upon their dynamics. In a study in which the rocket system is handled as a rigid-flexible coupling system, it is modeled as a combination of a vehicle, yaw body, pitch body, and launch tube [3]. Also, the dynamic behavior of a launcher-missile system is

*Corresponding Author: bulent.ozkan@tubitak.gov.tr

examined by regarding it on a movable platform [4]. Despite this fact, a lot of theoretical and practical studies come into the picture when robotic manipulators become the main concern. Actually, regarding their mechanical configuration generally combined of two articulated links, launchers are nothing but two-degree-of-freedom serial robot manipulators [5,6].

In this study, the considered launcher is described and the relevant equations of motion are derived for its azimuth and elevation planes. Here, the system is treated as a two-degree-of-freedom robot manipulator and the well-known Newton-Euler method is utilized in modeling the system dynamics. The final equation used to design the corresponding control system is found out by adding the effects of the actuation and transmission parameters for the electromechanical actuation system [7]. As the control approaches, the computed torque method with the PID (proportional, integral, and derivative) control action, computed torque method with the sliding mode control, and cascaded control algorithm based on the computed torque and sliding mode schemes are considered [8,9]. The mentioned three different control structures are applied upon the launcher in order to make the accurate control of its angular position under the diverting effects of the parameter. Consequently, the related computer simulations are performed and the attained results are compared.

2. DYNAMIC MODELING OF THE LAUNCHER

As mentioned above, rocket or missile launchers have two degrees of freedom which correspond to the azimuth and elevation axes. In physical sense, the azimuth axis defines the yaw motion of the moving part of the launcher while the elevation axis indicates its angular motion in the pitch plane [10,11].

In the given launcher configuration, a sleewing gear having the same diameter as the lateral size of the launcher is placed on the azimuth plane and it can freely rotate over a large bearing on the moving part. The sleewing gear is excited by means of a pinion gear fixed on the assembly. The reduction ratio between the pinion and servo electric motor is adjusted by a gearbox. Here, the reference torque input of the system is supplied by means of the servo electric motor.

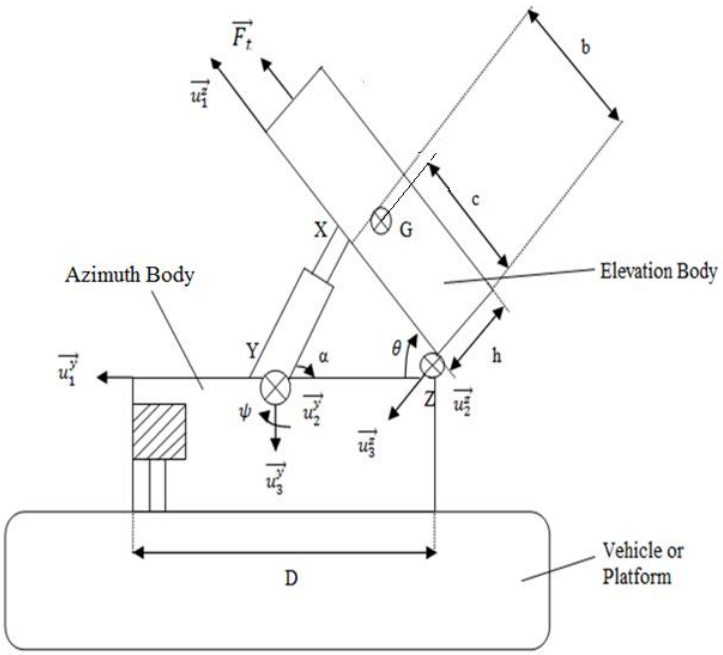

Figure 1. Schematic representation of the launcher.

The elevation plane is mounted onto the azimuth plane through two points that have rotational degree-of-freedom. The angular motion of the elevation body is supplied by a piston mechanism including a ballscrew used to convert rotational motion generated by a rotary actuator into translation.

The dynamic modeling of the launcher schematically represented in Figure 1 is carried out using the Newton-Euler method [7,11].

In Figure 1, as the label "Vehicle or Platform" denotes the launcher body, *D*, *G*, and $\overrightarrow{F_t}$ stand for the diameter of the sleewing gear, mass center of the system, and thrust force acting on the elevation body through the rocket or missile to be fired, respectively. Also, *b*, *c*, and *h* indicate the distance between the piston connection point and rear edge of the elevation body, the distance between the canter of mass and rear edge of the elevation body, and height of the elevation body, respectively. Moreover, α, θ, and ψ represent the angle between the piston and upper surface of the azimuth body, orientation of the elevation body with respect to the azimuth body which is to be controlled, and angle designated as the control variable for the azimuth body, respectively. Here, x, y, and z axes are indicated by unit vectors $\vec{u}_1$, $\vec{u}_2$, and $\vec{u}_3$ while $\vec{u}^y$ and $\vec{u}^z$ correspond to the azimuth and elevation axes.

As C_0, C_y, and C_z stand for the stationary reference frame, elevation body reference frame, and azimuth body reference frame, respectively, the coordinate transformation from the launcher platform to the elevation and azimuth planes can be defined in the following manner [1]:

$$C_0 \rightarrow {}_{0}^{1}R C_y \rightarrow {}_{1}^{2}R C_z \tag{1}$$

In equation (1), the rotation matrices are given below [1]:

$${}_{0}^{1}\hat{R} = \begin{bmatrix} cos\psi & -sin\psi & 0 \\ sin\psi & cos\psi & 0 \\ 0 & 0 & 1 \end{bmatrix} \tag{2}$$

$${}_{1}^{2}\hat{R} = \begin{bmatrix} cos\theta & 0 & sin\theta \\ 0 & 1 & 0 \\ -sin\theta & 0 & cos\theta \end{bmatrix} \tag{3}$$

Since ${}^0\vec{w}_0 = 0$, ${}^0\dot{\vec{w}}_0 = 0$, and ${}^0\dot{\vec{v}}_0 = 0$ for the stationary platform, the angular velocity, angular acceleration, linear acceleration of points on the rotation axis of the azimuth body, and linear acceleration of the center of mass of the azimuth body are written sequentially in the following manner:

$${}^1\vec{w}_1 = \dot{\psi}\,\overrightarrow{u_3^y} \tag{4}$$

$${}^1\dot{\vec{w}}_1 = \ddot{\psi}\,\overrightarrow{u_3^y} \tag{5}$$

$${}^1\dot{\vec{v}}_1 = 0 \tag{6}$$

$${}^1\dot{\vec{v}}_{C_1} = 0 \tag{7}$$

Similar equations can be put for the elevation body as follows:

$$^2\vec{w}_2 = \dot{\psi}\ sin(\theta)\ \overrightarrow{u_1^z} + \dot{\psi}\ cos(\theta)\ \overrightarrow{u_3^z} + \dot{\theta}\ \overrightarrow{u_2^z} \tag{8}$$

$$^2\dot{\vec{w}}_2 = [\ddot{\psi}\ sin(\theta) + \dot{\theta}\dot{\psi}\ cos(\theta)]\ \overrightarrow{u_1^z} + [\ddot{\psi}cos(\theta) + \dot{\theta}\dot{\psi}\ sin(\theta)]\ \overrightarrow{u_3^z} + \ \ddot{\theta}\ \overrightarrow{u_2^z} \tag{9}$$

$$^2\dot{\vec{v}}_2 = \frac{1}{2}Dcos(\theta)\dot{\psi}^2\ \overrightarrow{u_1^z} - \frac{1}{2}D\ddot{\psi}\ \overrightarrow{u_2^z} + \frac{1}{2}Dsin(\theta)\dot{\psi}^2\ \overrightarrow{u_3^z} \tag{10}$$

$$^2\dot{\vec{v}}_{C_2} = [\frac{1}{2}\Big((-\dot{\psi}^2 vcos(\theta) - \dot{\theta}^2 c - \ddot{\theta}h)\Big)\ \overrightarrow{u_1^z}\Big) + \Big((\ddot{\psi}v - 2\dot{\theta}\dot{\psi}(hcos(\theta) + csin(\theta))\ \overrightarrow{u_2^z}\Big) + \Big((-\dot{\psi}^2 vsin(\theta) + \dot{\theta}^2 h - \ddot{\theta}c)\ \overrightarrow{u_3^z}\Big) \tag{11}$$

Expressions giving the total force terms acting on the elevation and azimuth bodies can be then established in the next two equations, respectively:

$$^2\overrightarrow{F_2} = \overrightarrow{F_t} + \overrightarrow{F_p} + \overrightarrow{F_z} + \overrightarrow{W_z} \tag{12}$$

$$^1\overrightarrow{F_1} = \overrightarrow{F_y} - \overrightarrow{F_p} - \overrightarrow{F_z} + \overrightarrow{W_y} \tag{13}$$

In the above equations, $\overrightarrow{F_y}$ and $\overrightarrow{F_z}$ stand for the reaction force vectors at points *Y* and *Z*, respectively. Also, $\overrightarrow{F_p}$, $\overrightarrow{W_y}$, and $\overrightarrow{W_z}$ show the lifting force exerted on the elevation body by the piston mechanism, weight of the azimuth body, and weight of the elevation body, respectively. More clearly, the reaction and lifting force vectors in equations (12) and (13) can be expressed in component-wise as given below:

$$\overrightarrow{F_t} = F_{t1}\overrightarrow{u_1^z} + F_{t2}\overrightarrow{u_2^z} + F_{t3}\overrightarrow{u_3^z} \tag{14}$$

$$\overrightarrow{F_z} = F_{z1}\overrightarrow{u_1^z} + F_{z2}\overrightarrow{u_2^z} + F_{z3}\overrightarrow{u_3^z} \tag{15}$$

$$\overrightarrow{F_y} = F_{y1}\overrightarrow{u_1^y} + F_{y2}\overrightarrow{u_2^y} + F_{y3}\overrightarrow{u_3^y} \tag{16}$$

Weight vectors can be written more explicitly in the following manner:

$$\overrightarrow{W_z} = m_z g cos(\theta)\overrightarrow{u_3^z} - m_z \sin(\theta)\overrightarrow{u_1^z} \tag{17}$$

$$\overrightarrow{W_y} = m_y g\overrightarrow{u_3^y} \tag{18}$$

where m_z and m_y denote the masses of the elevation and azimuth bodies while g represents the gravity.

Additionally, the forthcoming expressions can be extracted for α and $\overrightarrow{F_p}$ from Figure 1:

$$\alpha = tan^{-1}[\frac{bsin(\theta)}{(\frac{D}{2}) - bcos(\theta)}] \tag{19}$$

$$\overrightarrow{F_p} = -F_p\ cos(\alpha - \theta)\ \overrightarrow{u_1^z} + F_p\ sin(\alpha - \theta)\overrightarrow{u_3^z} \tag{20}$$

Newton equation for the elevation body becomes as follows:

$$^{2}\vec{F}_2 = m_Z \, ^{2}\dot{\vec{v}}_{C_2} \tag{21}$$

Substituting equations (14), (15), (17), and (20) into equation (12) and then plugging equation (11) into equation (21), the expressions come into the picture in three axes:

$$F_{t1} + F_{z1} - F_p\, cos(\alpha - \theta) - m_z \sin(\theta) = \frac{m_z}{2}\left[\left(-\dot{\psi}^2 v cos(\theta) - \dot{\theta}^2 c - \ddot{\theta} h\right)\right] \tag{22}$$

$$F_{t2} + F_{z2} = \frac{m_z}{2}\left[(\ddot{\psi} v - 2\dot{\theta}\dot{\psi}(h cos(\theta) + c sin(\theta))\right] \tag{23}$$

$$F_{t3} + F_{z3} + F_p\, sin(\alpha - \theta)\overrightarrow{u_3^z} + m_z g cos(\theta) = \frac{m_z}{2}\left(-\dot{\psi}^2 v sin(\theta) + \dot{\theta}^2 h - \ddot{\theta} c\right) \tag{24}$$

where $v = c cos(\theta) - h sin(\theta) - D$.

Making the calculations for the azimuth body similar to the elevation body yields the scalar components in three axes:

$$F_{y1} - F_{z1}\cos(\theta) + F_{z3} sin(\theta) + F_p \cos(\alpha) = 0 \tag{25}$$

$$F_{y2} - F_{z2} = 0 \tag{26}$$

$$F_{y3} - F_{z1}\sin(\theta) - F_{z3}\cos(\theta) + F_p \sin(\alpha) + m_y g = 0 \tag{27}$$

From here, the Euler equation turns into the following form for the elevation body [1]:

$$^{2}\vec{N}_2 = {}^{C_2}\hat{I}_2 \, ^{2}\dot{\vec{w}}_2 + {}^{2}\vec{w}_2 \times {}^{C_2}\hat{I}_2 \, ^{2}\vec{w}_2 \tag{28}$$

Moments acting on the elevation body at point *Z* and the contributing vectors can be expressed as per the definitions in Figure 1 as listed below [1]:

$$\vec{N}_2 = \vec{r}_{N/Z} \times \overrightarrow{F_t} + \vec{r}_{X/Z} \times \overrightarrow{F_P} + \vec{r}_{G/Z} \times \overrightarrow{W_z} + \overrightarrow{M_z} + \overrightarrow{M_t} \tag{29}$$

$$\vec{r}_{N/Z} = c\overrightarrow{u_1^z} - \frac{h}{2}\overrightarrow{u_3^z} \tag{30}$$

$$\vec{r}_{X/Z} = b\overrightarrow{u_1^z} \tag{31}$$

$$\vec{r}_{G/Z} = \frac{c}{2}\overrightarrow{u_1^z} - \frac{h}{2}\overrightarrow{u_3^z} \tag{32}$$

$$\overrightarrow{M_z} = M_{z1}\overrightarrow{u_1^z} + M_{z2}\overrightarrow{u_2^z} + M_{z3}\overrightarrow{u_3^z} \tag{33}$$

$$\overrightarrow{M_t} = M_{t1}\overrightarrow{u_1^z} + M_{t2}\overrightarrow{u_2^z} + M_{t3}\overrightarrow{u_3^z} \tag{34}$$

$$^{C_2}\hat{I}_2 = J_{z11}\overrightarrow{u_1^z u_1^z} + J_{z22}\overrightarrow{u_2^z u_2^z} + J_{z33}\overrightarrow{u_3^z u_3^z} + \mathrm{J_{z13}}\overrightarrow{\mathrm{u_1^z u_3^z}} + \mathrm{J_{z13}}\overrightarrow{\mathrm{u_3^z u_1^z}} \tag{35}$$

where $\vec{M}_z$, $\vec{M}_t$, and ${}^{C_2}\hat{I}_2$ represent the reaction moment acting at point *Z*, thrust moment occurring at point *Z* due to the firing of the rocket, and moment of inertia dyadic for the elevation body, respectively.

Putting equations (8), (9) and (35) into equation (28) results in the next vector expression:

$$ {}^2\vec{N}_2 = \left(-\ddot{\psi}(J_{z11}\sin(\theta) - J_{z13}\cos(\theta)) - \dot{\theta}\dot{\psi}\cos(\theta)(J_{z11} + J_{z22} + J_{z33}) - 2J_{z13}\sin(\theta)\right)\overrightarrow{u_1^z} + \left(J_{z22}\ddot{\theta} + \dot{\psi}^2\sin(\theta)\cos(\theta)(J_{z33} - J_{z11}) - J_{z13}\dot{\psi}\cos(2\theta)\right)\overrightarrow{u_2^z} + (\ddot{\psi}(J_{z33}\cos(\theta) - J_{z13}\sin(\theta)) + \dot{\theta}\dot{\psi}\sin(\theta)(J_{z11} - J_{z22} - J_{z33}) - 2J_{z13}\dot{\theta}\dot{\psi}cos(\theta))\overrightarrow{u_3^z} \quad (36)$$

Matching the equation obtained by substituting equations (30) through (34) with equation (29) and equation (36), the following three scalar expressions arise:

$$ \frac{h}{2}F_{t2} + M_{z1} + M_{t1} = -\ddot{\psi}(J_{z11}\sin(\theta) - J_{z13}\cos(\theta)) - \dot{\theta}\dot{\psi}\cos(\theta)(J_{z11} + J_{z22} + J_{z33}) - 2J_{z13}\sin(\theta) \quad (37)$$

$$ -cF_{t3} - \frac{h}{2}F_{t1} - bF_P\,sin(\alpha - \theta) + \frac{1}{2}m_z g(hsin(\theta) - ccos(\theta)) + M_{z2} + M_{t2} = J_{z22}\ddot{\theta} + \dot{\psi}^2\sin(\theta)\cos(\theta)(J_{z33} - J_{z11}) - J_{z13}\dot{\psi}\cos(2\theta) \quad (38)$$

$$ cF_{t2} + M_{z3} + M_{t3} = \ddot{\psi}(J_{z33}\cos(\theta) - J_{z13}\sin(\theta)) + \dot{\theta}\dot{\psi}\sin(\theta)(J_{z11} - J_{z22} - J_{z33}) - 2J_{z13}\dot{\theta}\dot{\psi}\cos(\theta) \quad (39)$$

Euler equation and moment of inertia dyadic can be given for the azimuth body as follows:

$$ \overrightarrow{M_y} = M_{y1}\overrightarrow{u_1^y} + M_{y2}\overrightarrow{u_2^y} + M_{y3}\overrightarrow{u_3^y} \quad (40)$$

$$ {}^{C_1}\hat{I}_1 = J_{y11}\overrightarrow{u_1^y}\overrightarrow{u_1^y} + J_{y22}\overrightarrow{u_2^y}\overrightarrow{u_2^y} + J_{y33}\overrightarrow{u_3^y}\overrightarrow{u_3^y} \quad (41)$$

Similar to the elevation body, the three scalar equalities are derived for the azimuth body in the next fashion:

$$ M_{y1} - M_{z1}\cos(\theta) - M_{z3}\sin(\theta) = 0 \quad (42)$$

$$ M_{y2} - M_{z2} - \frac{D}{2}(F_{z1}\sin(\theta) + F_{z3}\cos(\theta)) = 0 \quad (43)$$

$$ T_M + M_{y3} - J_{y33}\ddot{\psi} + \frac{D}{2}F_{z2} - M_{z1}\sin(\theta) - M_{z3}\cos(\theta) = 0 \quad (44)$$

where M_y and T_M stand for the reaction moment acting at point *Y* and moment applied by the pinion on the sleewing gear.

Regarding all the scalar expressions derived above, the equations of motion for the elevation and azimuth bodies can be treated from equations (38) and (44) by considering the intermediate definitions made in equations (45) through (50) as finalized in equations (51) and (52), respectively:

$$J_m = \sin(\theta)\cos(\theta)(J_{z33} - J_{z11}) - J_{z13}\dot{\psi}\cos(2\theta) \tag{45}$$

$$W_m = \frac{1}{2}m_z g[h\sin(\theta) - c\cos(\theta)] \tag{46}$$

$$M_{z2} = -B_z\dot{\theta} \tag{47}$$

$$J_R = J_{y33} + J_{z11}sin^2(\theta) + J_{z33}cos^2(\theta) + J_{z13}\sin(2\theta) - \frac{Dvm_z}{4} \tag{48}$$

$$J_D = \frac{Dvm_z}{4}[h\cos(\theta) + c\sin(\theta)] + (J_{z11} - J_{z33})\cos(\theta)\sin(\theta) - J_{z13} \tag{49}$$

$$M_{y3} = -B_y\dot{\psi} \tag{50}$$

$$J_{z22}\ddot{\theta} + B_z\dot{\theta} + W_m + J_m\dot{\psi}^2 = -cF_{t3} - \frac{h}{2}F_{t1} - bF_P\, sin(\alpha - \theta) + M_{t2} \tag{51}$$

$$J_R\ddot{\psi} + B_y\dot{\psi} + 2J_D\dot{\theta}\dot{\psi} = T_M + \frac{1}{2}F_{t_2}[2c\cos(\theta) - h\sin(\theta) - D] - M_{t_1}\sin(\theta) + M_{t_3}\cos(\theta) \tag{52}$$

where B_y and B_z indicate the viscous friction coefficients between the pinion and sleewing gear in the azimuth body, and between the nut and screw of the ballscrew in the elevation body, respectively.

3. DESIGN OF THE CONTROL SYSTEM FOR THE LAUNCHER

For the rocket launcher considered, the control system is expected to fulfil the forthcoming essential functions:

- To orient the elevation body carrying the pod loaded by rockets and azimuth body over which the elevation body is mounted precisely to predetermined positions,

- To maintain the present angular positions of the elevation and azimuth bodies during rocket firing,

- To damp the oscillations occurring on the elevation and azimuth bodies right after the rocket firing as soon as possible,

- To minimize the diverting effect of the thrust generated by the rockets in firing and parameter uncertainties.

In a previous work dealing with the control of a rocket launcher, an adaptive computed torque algorithm is proposed along with the PID action in order to satisfy both performance and stabilization criteria [7,10]. Here, the computed torque approach is handled in two different configurations with PID and sliding mode control strategies.

The differential equations of motion of the launcher under consideration can be expressed in matrix form as follows [1]:

$$\widehat{M}(\vec{q})\ddot{\vec{q}} + \vec{N}\left(\vec{q}, \dot{\vec{q}}\right) + \vec{\tau}_d = \vec{\tau} \tag{53}$$

where $\widehat{M}(\vec{q})$, $\widehat{N}\left(\vec{q}, \dot{\vec{q}}\right)$, $\vec{\tau}_d$, and $\vec{\tau}$ denote the inertia matrix, vector involving the Coriolis, centrifugal, gravity, and frictional effects, vector of disturbing torques, and vector of the control torques, effectively.

The vector of the error variables and its successive time derivatives can be defined in the following sequence:

$$\vec{e}(t) = \vec{q}_d(t) - \vec{q} \tag{54}$$

$$\dot{\vec{e}} = \dot{\vec{q}}_d - \dot{\vec{q}} \tag{55}$$

$$\ddot{\vec{e}} = \ddot{\vec{q}}_d - \ddot{\vec{q}} \tag{56}$$

where $\vec{q}$, $\dot{\vec{q}}$, and $\ddot{\vec{q}}$ denote the vector of the control variables and its first and second time derivatives, $\vec{q}_d(t)$, $\dot{\vec{q}}_d$, and $\ddot{\vec{q}}_d$ represent the vector of the desired (reference) control variables and its successive time derivatives.

Picking up $\ddot{q}$ from equation (53) and putting it into equation (55), the next expression comes into the picture:

$$\ddot{\vec{e}} = \ddot{\vec{q}}_d + [\widehat{M}(\vec{q})]^{-1}[\vec{N}\left(\vec{q}, \dot{\vec{q}}\right) + \vec{\tau}_d - \vec{\tau}] \tag{57}$$

Defining the second time derivative of the error term as the control input, equation (57) turns into the following form:

$$\vec{u} = \ddot{\vec{q}}_d + [\widehat{M}(\vec{q})]^{-1}[\vec{N}\left(\vec{q}, \dot{\vec{q}}\right) + \vec{\tau}_d - \vec{\tau}] \tag{58}$$

Thus, the torque term can be calculated from equation (58) as per the computed torque method as follows:

$$\vec{\tau} = \widehat{M}(\vec{q})\left(\ddot{\vec{q}}_d - \vec{u}\right) + \vec{N}\left(\vec{q}, \dot{\vec{q}}\right) + \vec{\tau}_d \tag{59}$$

3.1. Computed Torque Method with PID Action

If the control variable ($u_1 = F_P$) is taken out of equation (51), the equation below occurs for the elevation body [12,13]:

$$u_1 = F_P = \frac{1}{-b\,sin(\alpha-\theta)}(-cF_{t3} - \frac{h}{2}F_{t1} + M_{t2} + W_m + J_m\dot{\psi}^2 + B_z\dot{\theta} + J_{z22}u_{1PID}) \tag{60}$$

In equation (60), the definitions given below are made:

$$u_{1PID} = \ddot{\theta}_d + 2\zeta_1\omega_{n1}\dot{e}_1 + {\omega_{n1}}^2 e_1 \tag{61}$$

$$e_1 = \theta_d - \theta \tag{62}$$

$$\dot{e}_1 = \dot{\theta}_d - \dot{\theta} \tag{63}$$

$$\ddot{e}_1 = \ddot{\theta}_d - \ddot{\theta} \tag{64}$$

$$\ddot{\theta} = u_{1PID} \tag{65}$$

where ω_{n1} and ζ_1 stand for the natural frequency and damping ratio of the elevation body, respectively.

Inserting equation (65) into equation (61) and then taking equation (64) into consideration in the resulting equation, the error dynamics happens to be in the next fashion:

$$\ddot{e_1} + 2\zeta_1\omega_{n1}\dot{e}_1 + {\omega_{n1}}^2 e_1 = 0 \tag{66}$$

In a similar manner, the control input and error dynamics equations can be written for the azimuth body for which T_M (= u_2) is chosen as the control variable:

$$u_2 = T_M = -\frac{1}{2}F_{t_2}[2ccos\theta - hsin\theta - D] + M_{t_1}sin\theta - M_{t_3}cos\theta + +2J_D\dot{\theta}\dot{\psi} + B_y\dot{\psi} + J_R u_{2PID} \tag{67}$$

$$J_R\ddot{\psi} = J_R u_{1PID} \tag{68}$$

$$\ddot{\psi} = u_{2PID} \tag{69}$$

$$u_{2PID} = \ddot{\psi}_d + 2\zeta_2\omega_{n2}\dot{e}_2 + {\omega_{n2}}^2 e_2 \tag{70}$$

$$\ddot{e_2} + 2\zeta_2\omega_{n2}\dot{e}_2 + {\omega_{n2}}^2 e_2 = 0 \tag{71}$$

where ω_{n2} and ζ_2 stand for the natural frequency and damping ratio of the azimuth body, respectively and $e_2 = \psi_d - \psi$.

Hence, the control torques (τ_1 and τ_2) can be designated for the elevation and azimuth bodies by regarding the PID action in the next two expressions, respectively:

$$\tau_1 = M_1\left(\ddot{\theta}_d - u_{1PID}\right) + N_1\left(\vec{q}, \dot{\vec{q}}\right) \tag{72}$$

$$\tau_2 = M_2\left(\ddot{\psi}_d - u_{2PID}\right) + N_2\left(\vec{q}, \dot{\vec{q}}\right) \tag{73}$$

where M_1 and M_2 stand for the first and second components of $\widehat{M}(\vec{q})$ on the main diagonal, respectively. Also, N_1 and N_2 denote the first and second elements of $\vec{N}\left(\vec{q}, \dot{\vec{q}}\right)$, respectively.

3.1. Computed Torque Method with Sliding Mode Controller

In order to make the system robust against parameter uncertainties and external disturbing effects, the performance of the control system based on the computed torque structure can be improved by supplementing it with the sliding mode control rather than the PID action. In this sense, the vector of the equivalent sliding mode control input ($\vec{u}_{smc}$) can be designated in the following manner [8]:

$$\vec{u}_{smc} = \widehat{M}\ddot{\vec{e}} + \hat{B}\dot{\vec{e}} \tag{74}$$

where $\widehat{M} = \widehat{M}(\vec{q})$ and $\hat{B} = \begin{bmatrix} B_y & 0 \\ 0 & B_z \end{bmatrix}$.

In equation (74), error terms are defined as given below:

$$\begin{cases} \vec{e}_1 = \vec{e} \\ \vec{e}_2 = \dot{\vec{e}} \end{cases} \Rightarrow \begin{matrix} \dot{\vec{e}}_1 = \vec{e}_2 \\ \dot{\vec{e}}_2 = -\hat{M}^{-1}\hat{B}\vec{e}_2 + \hat{M}^{-1}\vec{u}_{smc} \end{matrix} \tag{75}$$

The corresponding sliding surface (σ) can be established along with its first time derivative as follows [8]:

$$\vec{\sigma} = \vec{e}_2 + \hat{C}\vec{e}_1 \tag{76}$$

$$\dot{\vec{\sigma}} = \dot{\vec{e}}_2 + \hat{C}\dot{\vec{e}}_1 \tag{77}$$

where $\hat{C}$ stands for the matrix involving the sliding surface parameters.

Plugging equation (75) into equation (77) produces the forthcoming expression:

$$\dot{\vec{\sigma}} = -\hat{M}^{-1}\hat{B}\vec{e}_2 + \hat{M}^{-1}\vec{u}_{smc} + \hat{C}\vec{e}_2 \tag{78}$$

Here, $\vec{u}_{smc}$ can be assigned as

$$\vec{u}_{smc} = \hat{M}[\hat{M}^{-1}\hat{B}\vec{e}_2 + \hat{C}\vec{e}_2 + \hat{k}sgn(\vec{\sigma})] \tag{79}$$

The error terms are set in the following form by regarding equation (75):

$$\vec{e}_2 = \dot{\vec{e}}_1 = \dot{\vec{e}} = \begin{bmatrix} \dot{e}_y \\ \dot{e}_z \end{bmatrix} = \begin{bmatrix} \dot{\theta} - \dot{\theta}_d \\ \dot{\psi} - \dot{\psi}_d \end{bmatrix} \tag{80}$$

As $k_1$and k_2 are positive integer numbers, the matrix of controller gains ($\hat{k}$) can be defined as a 2×2 matrix together with the gain matrix $\hat{C}$ as

$$\hat{k} = \begin{bmatrix} k_1 & 0 \\ 0 & k_2 \end{bmatrix} \tag{81}$$

$$\hat{C} = \begin{bmatrix} \omega_{n1} & 0 \\ 0 & \omega_{n2} \end{bmatrix} \tag{82}$$

Substituting equation (82) into equation (77) results in the vector expression below:

$$\vec{\sigma} = \begin{bmatrix} \sigma_1 \\ \sigma_2 \end{bmatrix} = \begin{bmatrix} \dot{e}_y + C_1 e_y \\ \dot{e}_z + C_2 e_z \end{bmatrix} \tag{83}$$

where $C_1=\omega_{n1}$ and $C_2=\omega_{n2}$.

Further, equation (79) can be divided into its components corresponding to the elevation and azimuth bodies as follows:

$$u_{smc1} = M_1[(\hat{M}^{-1})_1 B_y e_x + C_1 e_y + k_1 sgn(\sigma_1)] \tag{84}$$

$$u_{smc2} = M_2[(\hat{M}^{-1})_2 B_z e_y + C_2 e_z + k_2 sgn(\sigma_2)] \tag{85}$$

where $\left(\widehat{M}^{-1}\right)_i$ denotes the component of matrix $\widehat{M}^{-1}$ on the i[th] row of its main diagonal for i=1 and 2.

Eventually, obeying equations (72) and (73), the control torques are composed for both of the bodies in accordance with the computed torque method with the sliding mode approach in the following fashion:

$$\tau_1 = M_1\left(\ddot{\theta}_d - u_{1PID} - u_{smc1}\right) + N_1(q, \dot{q}) \tag{86}$$

$$\tau_2 = M_2\left(\ddot{\psi}_d - u_{2PID} - u_{smc2}\right) + N_2(q, \dot{q}) \tag{87}$$

3.3. Cascaded Control Method based on Computed Torque and Sliding Mode Control Methods

In order to improve the stabilization capability of the launcher control system, it is a viable way to construct a cascaded control structure. In this scheme whose representative block diagram is given in Figure 2 for the elevation body, the inner loop attempts to "regulate" the fluctuations on the angular speed of the considered body due to disturbances and parameter uncertainties. Here, a control structure based on the computed torque and sliding mode control (SMC) approach is designed for the inner loop. Also, the stability of the proposed approach is guaranteed by regarding the sliding-surface-based Lyapunov function [1]. Accordingly, the outer loop with a PID controller is responsible of tracking the desired values of the control variable (orientation angle). The governing equations of the mentioned control systems are same as given in the preceding two sections. In Figure 2, Theta_d and Theta denote the desired and actual values of the orientation angles of the elevation body (θ) while Theta_d_dot and Theta_dot represent the desired and actual values of the time derivatives of θ, respectively.

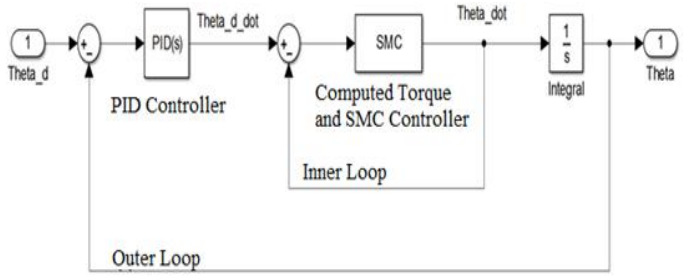

Figure 2. Cascaded control system for the launcher.

4. COMPUTER SIMULATIONS

The relevant computer simulations are performed in the MATLAB® SIMULINK® environment by considering the parameter values submitted in Table 1.

Table 1. Numerical values of parameters for simulations

Parameters	Numerical Values	Parameters	Numerical Values
b, c, and h	0.25 m	J_{z13}	1.5625 kg·m^2
D	0.5 m	B_y and B_z	0.01 N·m·s/rad
m_y and m_z	50 kg	ω_{n1} and ω_{n2}	20 Hz
$J_{z11}$and J_{z33}	1.3 kg·m^2	ζ_1 and ζ_2	0.707
J_{z22}	0.5 kg·m^2	k_1 and k_2	2000
F_{t2}, F_{t3}, and M_{t1}	0	F_{t1}	-50000 N

M_{t2}	10000 N·m	M_{t3}	5000 N·m

In the computer simulations, the elevation and azimuth bodies of the launcher are respectively steered from zero to 60 and 45˚, respectively. In the first case, it is assumed that the thrust force of firing munition does not affect the system. Using with relevant controller, the bodies are tried to bring their defined positions accurately.

Moreover, the impact effect caused by the firing thrust is added to the launcher when the response time reaches the steady state. The time range to reach the steady state is between 0.24 and 0.28 s. At 40 ms, impact effect is applied to the bodies to simulate the effect caused by the munition firing. Moreover, the total time of simulations is kept to be 0.5 s. The simulations are done with 25000 N·m disturbance torque at the relevant time due to thrust effect. The performance characteristics of the proposed three control system algorithms are compared by accounting the uncertainties 10% more, 10% less, and 20% more for the parameters given in Table 1. The attained values for the positioning errors for the proposed control systems are submitted in Table 2 under the thrust effect.

Table 2. Positioning errors for the proposed control systems under the thrust effect (°)

Body	**Parameter Uncertainty Level (%)**	**Type of the Control System**		
		Computed Torque Method with PID Action	**Computed Torque Method with Sliding Mode Controller**	**Cascaded Control Method based on Computed Torque and Sliding Mode Control Methods**
Elevation	0	9	8	5
	10	10	9	6
	-10	8	7	4
	20	11	10	6
Azimuth	0	1	0.3	0
	10	1.1	0.4	0
	-10	0.9	0.3	0
	20	1.2	0.5	0

Examining the data acquired from computer simulations as tabulated in Table 2, it can be concluded that the cascaded control system yields the smallest positioning error values at steady state. In this sense, the control system with the computed torque and PID control action exhibits the highest values. Moreover, there exists a proportion between the amount of the parameter uncertainties and increment or decrement in the positioning error. Namely, for instance, as submitted in Table 2, when the parameter uncertainty is 10% more in both the elevation and azimuth bodies, there occur approximately 10% increments compared to the quantities obtained for the case disregarding the uncertainties in the positioning accuracy data. A similar trend comes into the picture in torque demands as well.

The angular position changes of the elevation and azimuth bodies are submitted in Figure 3 through Figure 8 for all three different control algorithms. In the labels of these figures, PID, SMC, and cascaded short-hand notations correspond to the controller with the computed torque and PID action, controller with the computed torque and sliding mode control strategy, and cascaded control system explained above, respectively.

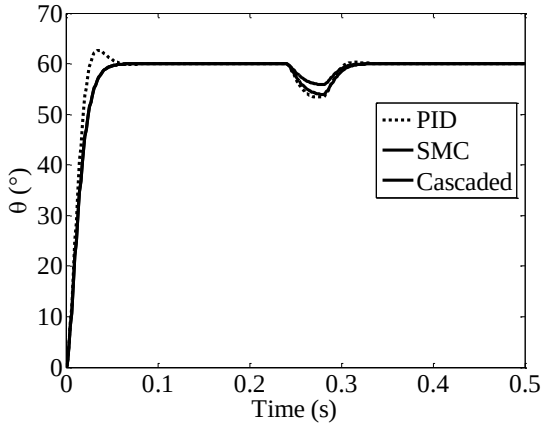

Figure 3. Change of the angular position of the elevation body in time for three different control system schemes (10% more parameter uncertainty).

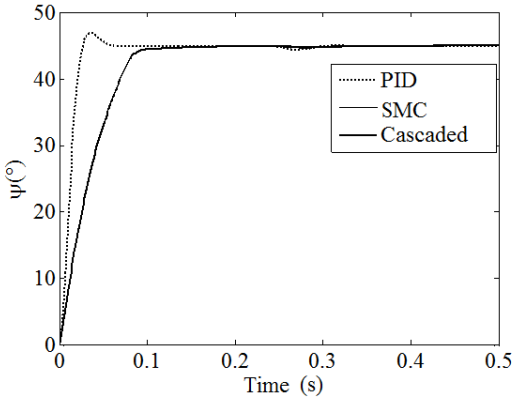

Figure 4. Change of the angular position of the azimuth body in time for three different control system schemes (10% more parameter uncertainty).

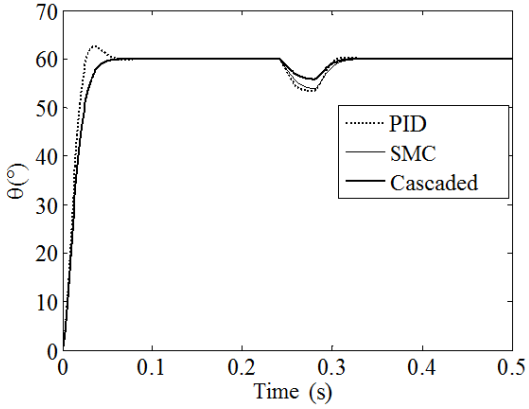

Figure 5. Change of the angular position of the elevation body in time for three different control system schemes (10% less parameter uncertainty).

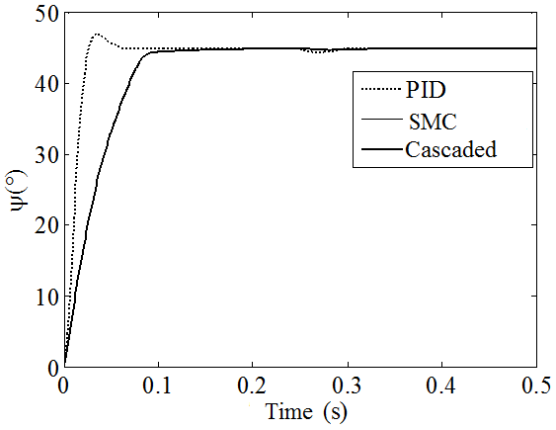

Figure 6. Change of the angular position of the azimuth body in time for three different control system schemes (10% less parameter uncertainty).

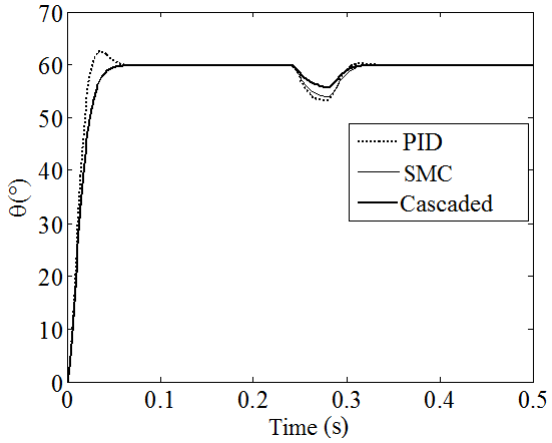

Figure 7. Change of the angular position of the elevation body in time for three different control system schemes (20% more parameter uncertainty).

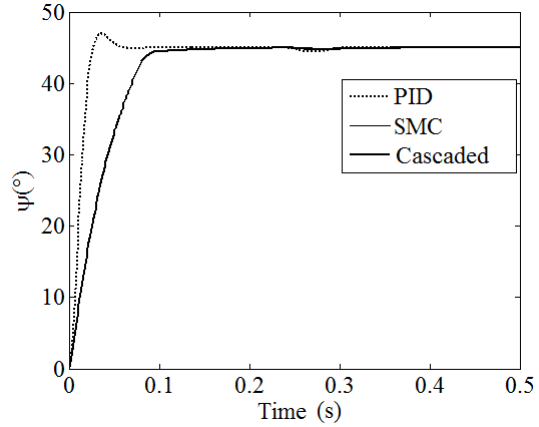

Figure 8. Change of the angular position of the azimuth body in time for three different control system schemes (20% more parameter uncertainty).

5. DISCUSSION AND CONCLUSION

As can be seen from the results of the computer simulations, the control system based on the computed torque and PID action becomes slower than the controller based on the computed torque and sliding mode control. The former controller also results in overshoot. The cascaded control system brings the elevation and azimuth bodies to their desired angular positions more accurately and slower than the other alternative control systems and it can diminish the negative effect of the thrust.

In order to diminish the amplitudes of the undesired oscillations caused by the thrust on the elevation and azimuth bodies, different values are assigned to the sliding mode gains. As a result of this trial, it is observed that the positioning accuracy gets better but the torque requirements grow for both of the bodies.

As per the computer simulations, the cascaded control system leads the smallest positioning error values at steady state whereas the computed torque and PID control action has the highest values. Also, the positioning error is consistent with the amount of the parameter uncertainties.

REFERENCES

[1] Kamişli H. Design of control systems for a launcher to reduce the thrust effect (thesis in Turkish with an abstract in English). MSc, Gazi University, Ankara, Turkey, 2015.

[2] Haug D, Wagner H. Active hardkill protection systems: analysis and evaluation of different system concepts. Technical Report, 2011.

[3] Zhang D, Xiao J. A dynamic model for rocket launcher with coupled rigid and flexible motion. Applied Mathematics and Mechanics 2005; 26: 5: 609-617.

[4] Dziopa Z, Krzysztofik I, Koruba Z. An analysis of the dynamics of a launcher-missile system on a movable base. Bulletin of the Polish Academy of Sciences, Technical Sciences, 2010; 58: 4: 645-650.

[5] Bingül Z, Küçük S. Robot Dinamiği ve Kontrolü. İstanbul, Turkey: Birsen Yayınevi, 2008.

[6] Dokumacı K. Mathematical modelling, PID and sliding mode control of a rocket launcher system. MSc, Gazi University, Ankara, Turkey, 2014.

[7] Kamişli H, Salamci MU, Özkan B. Elektromekanik eyletimli bir firlatma sisteminin itki etkisini en aza indirgeyecek şekilde denetimi. Otomatik Kontrol Ulusal Toplantısı (TOK), Denizli, Turkey, 2015.

[8] Utkin VI. Sliding Mode Control. Encylopedia of Life Support Systems (EOLSS), Control Systems, Robotics and Automation. Vol XIII, 2009.

[9] Utkin V, Guldner J, Shi J. Sliding Mode Control in Electromechanical Systems. USA: Taylor and Francis, 103-153, 271-302, 2009.

[10] Özkan B. Dynamic modeling and control of an electromechanically-actuated launcher (proceeding in Turkish with an abstract in English). Ulusal Makine Teorisi Sempozyumu, Erzurum, Turkey, 2013.

[11] Kamişli H, Salamci MU, Özkan B. Dynamic modeling of an electromechanically-actuated launcher. 17th International Carpathian Control Conference, Slovakia, 2016.

[12] Kamişli H, Salamci MU, Özkan B. Design of a cascaded control system for an electromechanically-actuated launcher to reduce the thrust effect. 17th International Carpathian Control Conference, Slovakia, 2016.

[13] Ogata K. Modern Control Engineering. 5th ed. New Jersey, USA: Pearson, 2010.